Technology developments towards the practical use of femtosecond laser micro-materials processing

Arnaud Zoubir, Lawrence Shah, Kathleen Richardson & Martin Richardson*
Laser Plasma Laboratory, School of Optics/CREOL, University of Central Florida

ABSTRACT

We describe several scenarios of basic femtosecond machining and materials processing that should lead to practical applications. Included are results on high through-put deep hole drilling in polymers and glasses in ambient air, and precision high speed micron-scale surface modification of materials.

Keywords: Femtosecond, micromachining, silicate, chalcogenide, composite materials, deep hole drilling, waveguides, gratings

1. INTRODUCTION

Femtosecond laser micromachining has become increasingly important in recent years for many fields including in micro-optics, micro-electronics, micro-biology and micro-chemistry. Laser ablation, because of its non-contact nature, allows the micromachining and surface patterning of materials with minimal mechanical and thermal deformation. It is now well known that for many of these applications the femtosecond regime offers advantages over the nanosecond regime. These advantages lie in its ability to deposit energy into a material in a very short time period, before thermal diffusion can occur. As a result, the heat-affected zone, where melting and solidification can occur, is significantly reduced. Smaller feature sizes, greater spatial resolution and better aspect ratios can hence be achieved.

Another advantage of femtosecond laser micromachining is its versatility in terms of both the materials to be processed and the type of processing. A variety of materials have been demonstrated to be suitable for femtosecond laser micromachining such as metals, semiconductors, polymers, oxide ceramics, silica aerogels, optical glasses and crystals… And a variety of processing has been done including the fabrication of photonic crystals[1], data storage, fabrication of waveguides[2], gratings and single mode couplers[3].

We present the femtosecond laser micromachining of different materials from three perspectives, (i) deep hole penetration in optical glasses and composite materials, (ii) the fabrication of gratings and (iii) the creation of waveguides, in ~~a~~ chalcogenide glass As_2S_3 thin films. We characterize the deep hole drilling by measuring the maximum laser penetration depth in a variety of glasses. We investigate the evolution of material expulsion as a function of the hole depth. We characterize waveguides and gratings fabricated by femtosecond laser writing using a standard interferometric microscope. Insight on the photorefractive mechanism caused by a femtosecond pulse is given by Raman spectra of guided light.

2. THEORETICAL BACKGROUND

2.1 Ablation mechanisms

To this date, the mechanisms that govern femtosecond laser ablation are not fully understood. Current understanding is approximately the following[4]: Bound and free electrons at the surface layer are excited via multi-photon absorption. Hot electrons are generated, the material becomes ionized and a plasma forms at the surface of the material. The energy is then transferred to the lattice through bond breaking and material expansion.

High-Power Laser Ablation IV, Claude R. Phipps, Editor, Proceedings of SPIE Vol. 4760 (2002)

Figure 1 – Schematic illustrating the difference between conventional (a) and femtosecond (b) micromachining

2.2 Advantages of the femtosecond regime

Because the processes described above are happening on a picosecond time scale, the thermal diffusion into the material is nearly negligible. The thermal relaxation is characterized by the thermal diffusion length D related to the pulse width τ_p by $D = \kappa\tau_p^{1/2}$, where κ is the thermal diffusivity of the material[5]. If D is shorter than the absorption length, the ablation precedes the thermal diffusion and the material does not have time to melt and resolidify. Better spatial resolutions can be achieved.

In addition, in the nanosecond regime, it is generally accepted that ablation begins with the ionization of surface carriers, which are typically defects or impurities[6]. Due to the non-uniform distribution of surface carriers in dielectrics, experiments have demonstrated that no precisely-defined laser-induced damage threshold exists for laser pulses longer than 10 ps. By contrast, ultrashort laser pulses (<200 fs), with target intensities often in excess of 10^{12} W/cm^2, are capable of freeing bound electrons via Multi-Photon Ionization (MPI). Thus, experiments have shown that the laser-induced damage threshold of an ultrashort laser pulse has a precise value corresponding to the onset MPI, which is completely determined by the ionization bandgap energy of the target material.

The reasons above make femtosecond micromachining an attractive technique for the fabrication of fine surface structures in transparent materials. In this paper, we demonstrate that femtosecond laser pulses from a regeneratively amplified Ti:Sapphire can be used to drill holes (≥1 mm in depth) with high aspect ratio (≥10:1) in transparent materials at atmospheric pressure.

3. DEEP HOLE DRILLING IN SILICATE GLASS

3.1 Experiment

We have investigated the laser ablation of two silicate glasses in three different laser ablation scenarios: with a femtosecond laser at 845 nm, with a nanosecond laser at 845 nm and with a nanosecond laser at 1064nm. In order to study the influence of the ionization bandgap on laser ablation, we use soda-lime glass (~5 eV) and 45%mol. PbO lead-silicate glass (~2.5 eV) as ablated materials[7]. Ablation is performed at atmospheric pressure in two regimes, below and above the air ionization threshold intensity, to gauge how air-ionization modifies the hole profile and material removal rate.

The femtosecond laser system is a Kerr-lens modelocked Ti:Sapphire oscillator regeneratively amplified by a flashlamp pumped Cr:LiSAF amplifier, able to produce 110 fs (FWHM) laser pulses with a Gaussian temporal profile at 845 nm. The second laser is the unseeded CrLiSAF regenerative amplifier, which produces long (60 ns) Q-switched pulses, at 845 nm, from which square 10 ns pulses are sliced using an

extra-cavity Pockels cell as an electro-optical pulse cutter. The third laser is a flashlamp pumped Q-switched Nd:YAG laser that produced 15 ns (FWHM) Gaussian-shaped laser pulses at 1064 nm. The laser parameters are listed in Table 1.

Each setup was identical, only differing in the laser source: The laser beam is expanded using a 4:1 telescope and filtered by an iris. It is then focused to a 100μm diameter spot onto the target using a fused silica plano-convex lens with a 20 cm focal length. After initial positioning, the focus spot was not moved during the ablation. The holes are drilled parallel to the long axis of thin polished glass plates.

Laser	Wavelength λ (nm)	Pulse Duration t_p Pulse Energy, E_p	Repetition Rate, R (Hz)	Focal Spot Diameter, D (μm)	Laser Fluence, F_p (J/cm^2)	Focal Intensity, I_p (W/cm^2)
Ti:Saph/ Cr:LiSAF	845	110 fs (FWHM) 1.5 mJ	5	100 (FW1/e^{2}M)	19.1	1.74x10^{14}
Cr:LiSAF	845	10 ns (FWHM) 4.0 mJ	5	100 (FW1/e^{2}M)	51.0	5.10x10^9
Nd:YAG	1064	15 ns (FWHM) 2.2 mJ	10	100 (FW1/e^{2}M)	28.0	1.87x10^9

Table 1 – Laser parameters

3.2 Results

Optical microscope images of the holes produced by 10^4 laser pulses in soda-lime silicate glass and PbO lead-silicate glass are shown in Figure 2 and 3.

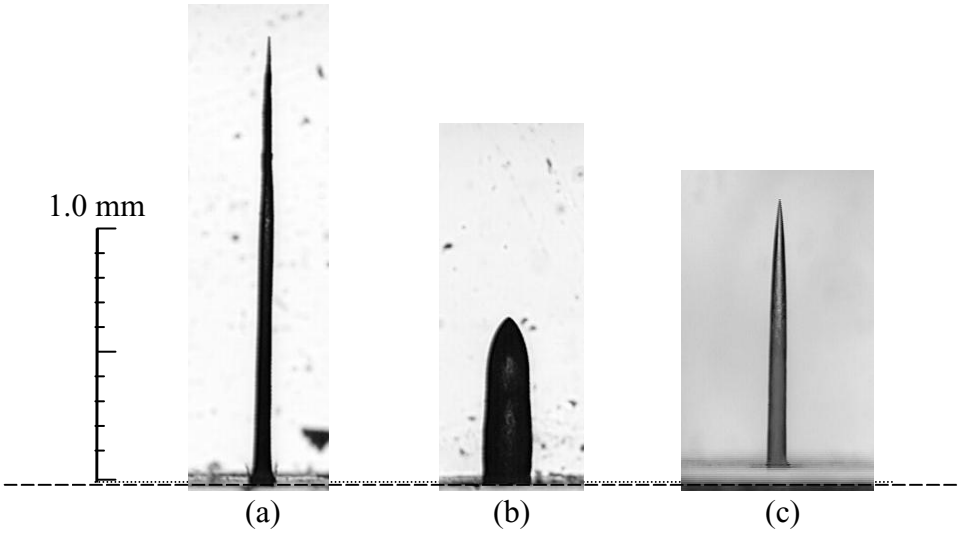

Figure 2: Hole profiles in soda-lime glass produced by 10^4 laser pulses
a) λ = 845 nm, t_p = 110 fs, E_p = 1.5 mJ, I_p = 1.74x10^{14} W/cm^2, F_p = 19.1 J/cm^2
b) λ = 845 nm, t_p = 10 ns, E_p = 4.0 mJ, I_p = 5.10x10^9 W/cm^2, F_p =51.0 J/cm^2
c) λ = 1064 nm, t_p = 15 ns, E_p = 2.2 mJ, I_p = 1.87x10^9 W/cm^2, F_p =28.0 J/cm^2

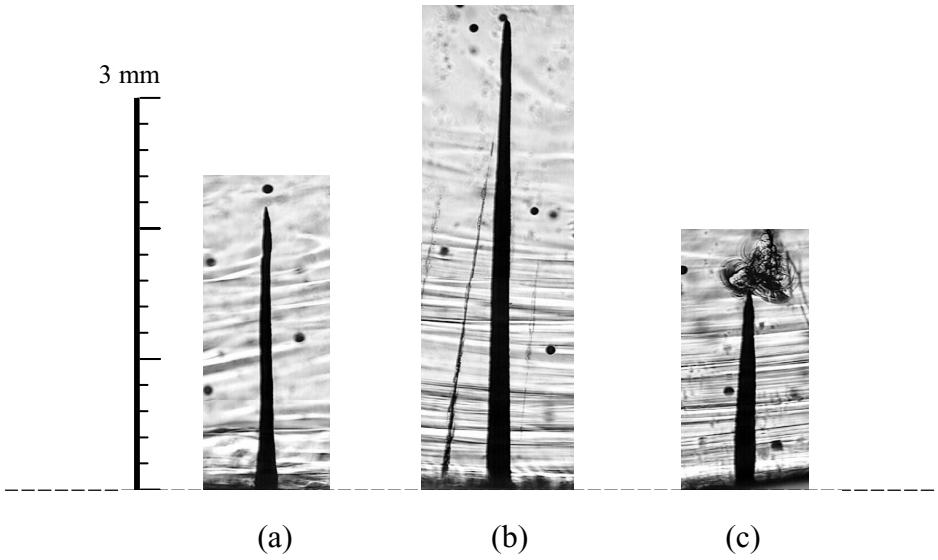

Figure 3: Hole profiles in 45% mol. lead silicate glass produced by 10^4 laser pulses
a) λ = 845 nm, t_p = 110 fs, E_p = 1.5 mJ, $I_p = 1.74 \times 10^{14}$ W/cm^2, F_p = 19.1 J/cm^2
b) λ = 845 nm, t_p = 10 ns, E_p = 4.0 mJ, $I_p = 5.10 \times 10^9$ W/cm^2, F_p =51.0 J/cm^2
c) λ = 1064 nm, t_p = 15 ns, E_p = 2.2 mJ, $I_p = 1.87 \times 10^9$ W/cm^2, F_p =28.0 J/cm^2

The overall penetration depth is significantly greater for PbO lead-silicate than for soda-lime silicate glass in the three different ablation scenarios due to a higher Z resulting in a higher electron density. In addition, there is a drastic difference in hole depth and width between Figure 2b and Figure 2c, which illustrates the variations in ablation mechanism and hole morphology obtained in the nanosecond regime at 845 nm and 1064 nm. Furthermore, in both materials, the femtosecond ablation is more energetically efficient as greater penetration depth are obtained with a smaller energy per pulse.

The same experiment was done in the femtosecond regime with fluences now sufficient to ionize the air. The fluence of the laser was increased by reducing the beam spot size from 100 μm to 75 μm. We compare the femtosecond laser ablation of the two silicate glasses below and above the air ionization threshold in Figure 4. Below air ionization threshold, the ablation rate remained constant over the tested range at ~0.2 μm/pulse for both glasses. Above threshold, the ablation rate rises up to ~0.5 μm/pulse and rapidly reduces down to ~0.05 μm/pulse (at ~1000 shots for soda-lime and ~5000 shots for PbO silicate glass). It can be seen that there is a striking increase in the ablation-rate for the PbO glass at higher intensities. There are number of possible explanations for this. Firstly, we know that the influence of the air ionization makes a change to the ablation rate[8]. However, the interaction physics with the higher Z glass could also be playing a role, and one cannot exclude the possible differences in material properties.

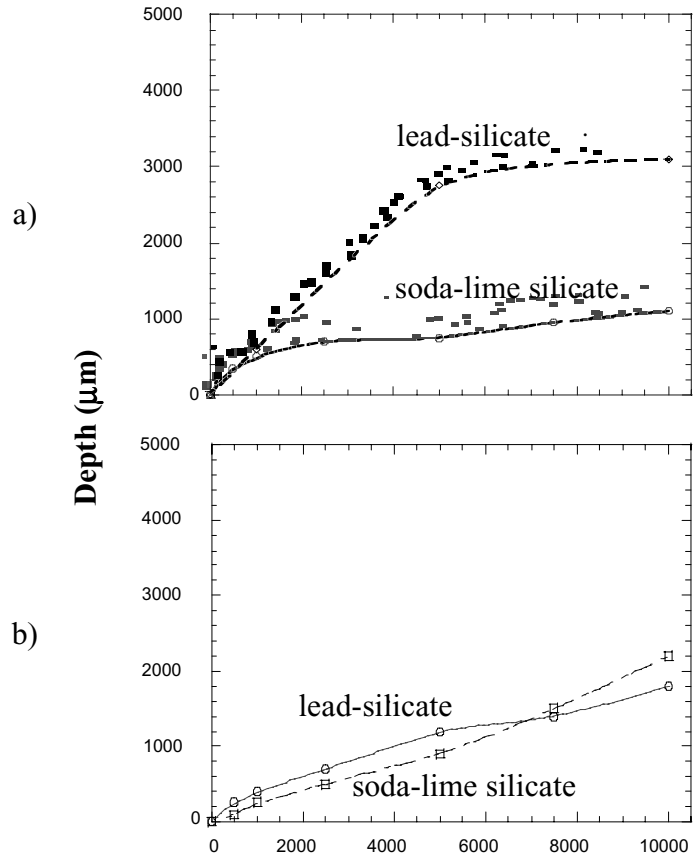

Figure 4: Laser penetration depth vs. number of incident laser pulses (t_p = 110 fs, λ = 845 nm, E_p = 1.5 mJ) given:
a) $I_p = 3.08 \times 10^{14}$ W/cm^2, F_p = 33.9 J/cm, and d = 75 μm (FW1/e^{2}M)
b) $I_p = 1.74 \times 10^{14}$ W/cm^2, F_p = 19.1 J/cm^2, and d = 100 μm (FW1/e^{2}M)

Optical probe images, taken during the laser material interaction above ionization threshold, revealed that after a certain depth is achieved, light starts to form a thin (~10 μm) hot filament confined inside the hole (Figure 5).

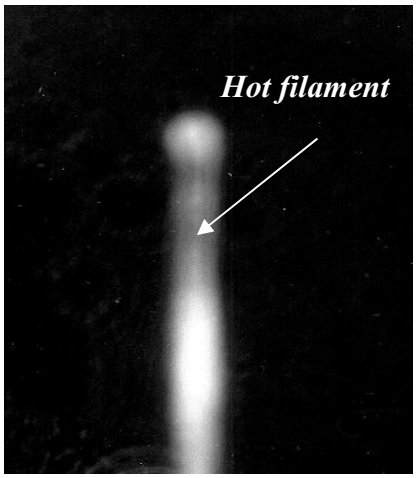

Figure 5 – Hot filament inside an ablated hole in lead silicate glass

High-intensity ultrashort laser pulses propagating in air have been observed to self-channel into light filaments exceeding the Raleigh length[9]. It is believed that a similar effect occurs because of evaporated material that remains temporarily confined in the hole, thus increasing the nonlinear index of refraction of the atmosphere. More evidence of this effect is present in Figure 6 where very sharp holes pointing in slightly different directions are shown at the tip of the hole both in lead silicate glass and As_2S_3, a chalcogenide glass. These pins could be attributed to ablation due to self-channeled single shots. Note that the individual pins or filaments in the material are uniformly ~ 100 μm long. In addition, it is important to note that the rollover in the ablation rate described above occurred earlier for PbO lead silicate than for soda-lime silicate. The presence of high Z elements (PbO) or particles of highly non linear material (As_2S_3) in the hole atmosphere can account for a higher nonlinear index of refraction, thus lowering the intensity threshold for self-focusing.

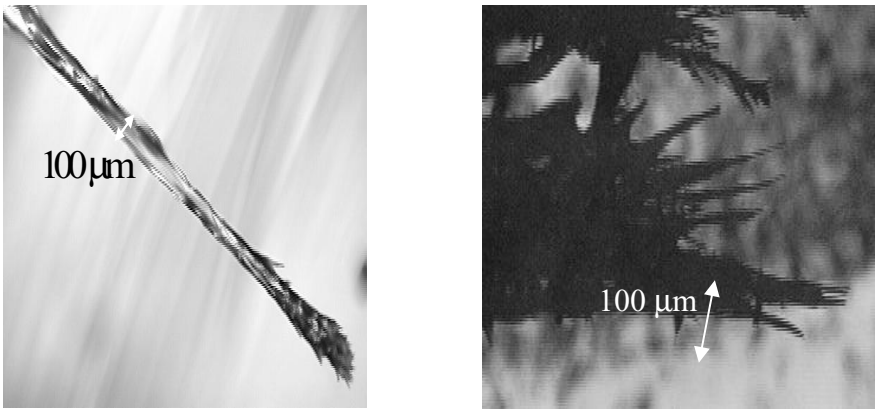

Figure 6 – Evidence of self-focusing in lead silicate and chalcogenide glass

4. HOLE DRILLING IN COMPOSITE MATERIAL

To further illustrate the hole morphology advantages and versatility of femtosecond ablation, ablation was performed on a 3mm thick graphite fiber composite material. Again ablation is done in both the nanosecond and femtosecond regime (Figure 7).

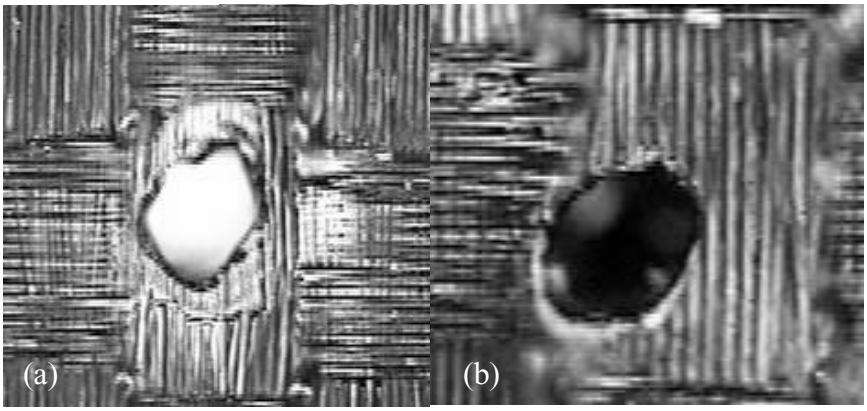

Figure 7 – 100x70 μm ablated hole in graphite fiber composite material
(a) Conventional nanosecond laser 1300 pulses with ~ 3.5 mJ/pulse
(b) 100 fs laser pulses in air, ~ 1 mJ/pulse

While the nanosecond regime yields dislocation of horizontal and vertical striations indicative of extent of heat-affected zone, the femtosecond regimes shows a clean, reproducible hole structure, without evidence of collateral surface damage. The difference in the size of the heat-affected zone is expected to be even greater in laminate materials where the heat caused by long pulses can only diffuse in two dimensions versus three in bulk material.

5. GRATING FABRICATION IN As_2S_3 CHALCOGENIDE GLASS THIN FILMS

Femtosecond lasers appear to be a promising tool for the microstructuring of optical materials. It was demonstrated that unamplified femtosecond lasers could produce optical breakdown and structural change in bulk transparent materials using tightly focused pulses of just 5 nJ[10].

5.1 Grating fabrication

Using an extended cavity unamplified Kerr-lens modelocked Ti:Sapphire laser, relief and volume gratings with a 20 μm period were fabricated on a 1.66 μm thick, As_2S_3 thin film. The laser emission has a spectral bandwidth of approximately 40 nm (FWHM) centered at 800 nm and a repetition rate of 28 MHz. An interferometric autocorrelation measured sub-50 fs pulse duration. The system has an average output power of 0.55 W and produces energies up to 20 nJ per pulse. The output of the laser was focused by a 15x, 0.28NA reflective objective onto a target attached to a 3D motorized translation system.
The sample was processed in two regimes: Firstly, the intensity was kept below the ablation threshold, generating a volume grating resulting from photoexpansion and an induced index change, as observed through an interferometric microscope. In the second regime, intensities *above* the ablation threshold produced a relief grating with grooves of 0.2 μm depth (Figure 8).

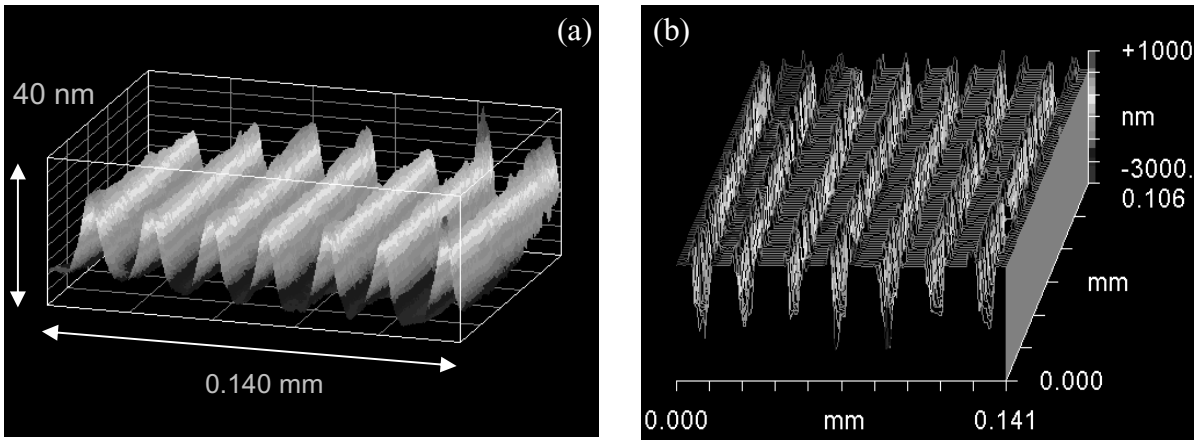

Figure 8 – Surface profile of (a) the phase and (b) relief grating on the As_2S_3 film produced with sub-50 fs laser pulses from the extended cavity unamplified Ti:Sapphire oscillator

5.2 Waveguide fabrication

Previous studies have linked bulk glass structural and optical property changes (photosensitivity) through Raman spectroscopy, showing that nonlinear absorption-induced index changes were linked to local bonding changes in As_2S_3[11]. Following this approach, waveguides over 1 cm in length and ~10 μm in diameter were fabricated in As_2S_3 thin films by direct transverse writing using the same umamplified Ti:Sapphire laser (Figure 9).

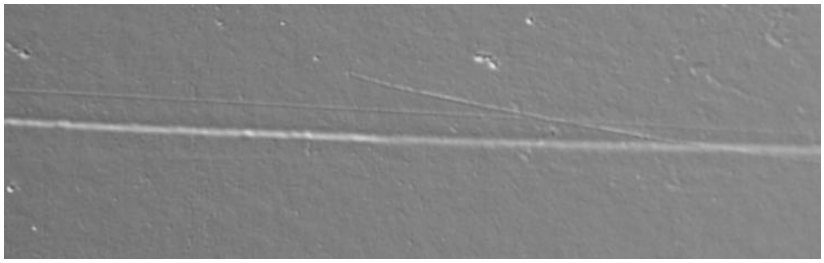

Figure 9 – Waveguide fabricated with the unamplified Ti:Sapphire laser

Further studies are underway including the measurement of the refractive index change by the refracted near-field technique. In addition, waveguide Raman spectroscopic measurements in the film will be compared to the previous results in bulk to confirm the molecular bond changes that give rise to the change of refractive index.
This technique has already established its ability to create complex waveguide structures in optical materials. For instance, directional couplers and 3D-waveguides were fabricated using a nanojoule laser in borosilicate glass[12] and soda-lime glass. With a reduced complexity of operation and an increased cost-effectiveness, nonlinear material processing with near-IR femtosecond pulses will be of great interest to optical communication systems manufacturers for miniaturization and integration of photonic devices.

6. CONCLUSION

This study has shown the ability of femtosecond material microprocessing to produce very fine surface structures and its versatility both in the type of processing and the type of materials to be processed. Comparison between the femtosecond and nanosecond regimes has shown one more time that finer, more energy-effective and more material-independent structuring could be obtained with femtosecond pulses.

REFERENCES

1. Sun, H.-B. ; Xu, Y.; Juodkazis, S.; Sun, K.; Watanabe, M.; Matsuo, S.; Misawa, H.; Nishii, J., "Arbitrary-lattice photonic crystals created by multiphoton microfabrication", *Optics Letters*, **Vol. 26**, Issue 6, pp. 325-327, 2001.

2. Hirao, K.; Miura, K., "Writing waveguides and gratings in silica and related materials by a femtosecond laser", *Journal of Non-Crystalline Solids*, **Vol. 239**, Issue 1-3, pp. 91-95, 1998.

3. Minoshima, K. ; Kowalevicz, A.M.; Hartl, I.; Ippen, E.P.; Fujimoto, J.G., "Photonic device fabrication in glass by use of nonlinear materials processing with a femtosecond laser oscillator", *Optics Letters*, **Vol. 26**, Issue 19, pp. 1516-1518, 2001.

4. Korte, F. ; Adams, S.; Egbert, A.; Fallnich, C.; Ostendorf, A.; Nolte, S.; Will, M.; Ruske, J.-P.; Chichkov, B.N.; Tunnermann et al., "Sub-diffraction limited structuring of solid targets with femtosecond laser pulses", *Optics Express*, **Vol. 7**, Issue 2, 2000.

5. Matthias, E. ; Reichling, M.; Siegel, J.; Kading, O.W.; Petzoldt, S.; Skurk, H.; Bizenberger, P.; Neske, E., "The influence of thermal diffusion on laser ablation of metal films*", Applied Physics A (Solids and Surfaces)*, **Vol. A58**, Issue 2, pp. 129-136, 1994.

6. N. Bloembergen. IEEE J. of Quantum Electron., **QE-10**, 375, 1974.

7. Schott Glass Technologies Inc., *Optical Glass Catalog*, 400 York Avenue, Duryea, Pennsylvania 18642.

8. L. Shah, Femtosecond *laser micro-machining of glasses and polymers in air*, Ph.D. Thesis, , University of Central Florida, Fall 2001.

9. Braun, A. ; Korn, G.; Liu, X.; Du, D.; Squier, J.; Mourou, G., "Self-channeling of high-peak-power femtosecond laser pulses in air", *Optics Letters*, **Vol. 20**, Issue 1, pp. 73-75, 1995.

10. Schaffer, C.B. ; Brodeur, A.; Garcia, J.F.; Mazur, E., "Micromachining bulk glass by use of femtosecond laser pulses with nanojoule energy", *Optics Letters*, **Vol. 26**, Issue 2 , pp. 93-95, 2001.

11. T. Cardinal, K. A. Richardson, H. Shim, A. Schulte, R. Beatty, K. Le Foulgoc, C. Meneghini, J. F. Viens, A. Villeneuve, "Non-linear optical properties of chalcogenide glasses in the system As-S-Se", *Journal of Non-Crystalline Solids*, **Vol. 256-257**, pp. 353-60, 1998.

12. , Streltsov, A.M. ; Borrelli, N.F., "Fabrication and analysis of a directional coupler written in glass by nanojoule femtosecond laser pulses", *Optics Letters*, **Vol. 26**, Issue 1, pp. 42-43, 2001.

* mrichard@mail.ucf.edu; phone 407 823 6819; fax 407 823 3570; School of Optics/CREOL, University of Central Florida, 4000 Central Florida Blvd., PO BOX 162700, Orlando FL 32816.